MULTIFRACTAL CROSS CORRELATION ANALYSIS BETWEEN AEROSOLS AND METEOROLOGICAL DATA

C. MARIN[1,2], C. STAN[1], L. PREDA[1], L. MARMUREANU[2], L. BELEGANTE[2], C. P. CRISTESCU[1]

[1]*Politehnica* University of Bucharest, Department of Physics,
313 Spl. Independentei, R0-060042, Bucharest, Romania
E-mails: cristina.stan@physics.pub.ro; constantin.cristescu@physics.pub.ro;
liliana.preda@physics.pub.ro
[2] National Institute for Research and Development in Optoelectronics
409 Atomistilor Str., Măgurele, 077125, CP MG5, Ilfov – Magurele, Romania
E-mails: cristina.marin@inoe.ro; belegantelivio@inoe.ro; mluminita@inoe.ro

Received November 16, 2017

Abstract. We perform a multifractal detrended cross-correlation analysis between the total concentration of particles from 0.5 to 20 microns, their mean radius and the average of some meteorological element: air temperature, wind speed, solar radiation, relative humidity and absolute pressure. Data are collected in a campaign of measurements performed from July until August 2016 in the Magurele area. Time series are simultaneously recorded with a resolution of 15 min. Multifractal characteristics are defined by the dependence of the Hurst exponents *versus* the fluctuation order and by the singularity spectra. Different types of correlations observed between aerosols concentration/radius and the meteorological parameters are quantitatively described by the parameters of the logistic function, as the best fitting of the Hurst exponents *versus* the fluctuations intensity.

Key words: aerosols, multifractal analysis, cross-correlation, Hurst exponent.

1. INTRODUCTION

Recent studies have proven that the presence of aerosols in the atmosphere has significant direct and indirect effects on air quality, climate, and rainfalls, things related to the phenomenon of global warming and the quality of life [1]. The impact produced by aerosols is related to their physical and chemical properties [2]. Some of the aerosol species (mainly anthropogenic ones) are known to inflict harmful effects on humans. There is a strong effort towards limiting the maximum concentration and enforce safety levels for the atmospheric micro and nanoparticles most hazardous to human health [3] and consequently, a large interest towards minimizing the uncertainties associated with data collection [3, 4].

Different approaches and methods have been developed for analyzing particle diameter sizes ranging from 10 nm to 10 μm [5]. Investigations on atmospheric aerosols, viruses, bacteria, and chemical agents, can be performed using high precision mass measurements for micro and nanoparticles [6]. Recent experiments and results seem to indicate that ion traps [7, 8] can be coupled to an Aerosol Mass Spectrometer to investigate atmospheric aerosol (nano)particles. Experimental setups based on multipole Paul traps enable confinement as well as qualitative investigation of atmospheric particles and aerosols [9].

In the last decades, an increasing attention has been paid to the quest for correlations and scaling behavior of nonstationary time series expressed as data sequences in physics, biology, medicine, earth sciences, econophysics and environmental sciences [10–15]. Environmentalists understand the importance of testing new methods of investigation and analysis of air pollution time-series and their relationship with respect to meteorological elements [16–19]. Different techniques based on mono- and multi-fractal box counting methods or by trend analysis were proposed for scaling the aerosol time-series [19, 20].

Multifractal formalism has been successfully applied for systems in environmental science, and it may also have great potential in modelling the cross-connection between air pollution and some meteorological factors [21–24]. Characteristics of fluctuations and cross-correlation trends between aerosols and local climate characteristics can be successfully investigated using the formalism of multifractal detrended cross-correlation MFDCCA [24]. In such framework we report long range correlations for total concentration of aerosols with dimensions ranging between 0.5 and 20 microns, their average concentration and some meteorological parameters, and we also compute the spectrum of fractal dimensions.

2. METHODOLOGY AND DATA COLLECTION

The MFDCCA formalism for computing the Hurst exponent and singularity spectrum follows some specific steps presented in detail in [13, 25]. The cross-correlated multifractal analysis is performed on aerosol data (total concentration (no/cm^3) and mean radius) and local meteorological characteristics: *air temperature* (Temp), *wind speed* (WS), *solar radiation* (SolRad), *relative humidity* (Hum) and *absolute pressure* (Pres).

All the data are collected in a campaign of measurements performed from July until August 2016 in the Măgurele area (44^o 21’ N, 26^o 02’ E), near Bucharest, Romania. Meteorological data representing the average air temperature (C), average wind speed (km/h), average solar radiation (W/m^2), average relative humidity [%] and average absolute pressure (hPa) are simultaneously measured at the same location.

Size distribution of aerosols, with diameters ranging between 0.5 and 20 μm, were measured using a TSI *Aerodynamic Particle Sizer* (APS) based on a *time-of-flight* (TOF) method. In the accelerated flow field, the time taken by the particle to travel between two concurrent laser beams is measured. The resulting particle acceleration rate is converted into a corresponding aerodynamic diameter, which is defined as a particle that has the same settling speed as a spherical particle with the density of $1 g \cdot cm^{-3}$, and thus essentially depends on the particle mass. In the APS, the aerosol and sheath flow rates are about 1 L and 4 L per minute, respectively. Inlet line losses associated to measurements are minimized using a vertically positioned moderately heated inlet. With properly calibrated inlet and aerosol flow rates, the aerodynamic sizing of the APS can be considered accurate.

The processed time series are simultaneously recorded with a resolution of 15 min.

3. RESULTS AND DISCUSSION

Figure 1 (upper panel) shows the dependence of the generalized Hurst exponent h on the order fluctuation q, for original data of total concentration of aerosol particles (squares) and the mean radius (open circles). The corresponding singularity spectra $f(\alpha)$ are shown in the lower panel of Fig. 1.

From the shape and extension of the curves, one can obtain significant information about the aerosol distribution and associated structure. The total concentration curve is larger in the domain of singularities compared to the mean radius spectrum. The left branches of the multifractal spectrum $f(\alpha)$, corresponding to positive values of the parameter q which describes regions of high fluctuations in concentration/radius, are shorter than those corresponding to the branch of negative q values. This means that the fractal dimensions range for high fluctuations is smaller compared to the case of small fluctuations, possibly due to the occurrence of aggregates.

As it is known, low values of $f(\alpha)$ characterize a rare occurrence of isolated peaks in a data sample, while higher values of $f(\alpha)$ are typical for a more frequent and dense appearance of high data values. Similar to the case of multifractal curves, for most of the singularity exponent *alpha* range, the curve for the cross-correlation spectrum is located between the curves corresponding to the singularity spectra of the two independent data sets.

Figure 2 shows the generalized Hurst exponents H_12 for the cross-correlation between the total concentration and the meteorological parameters (upper panel), and between the mean radius and the meteorological parameters (lower panel). The curves for different parameters are explained in each figure. As one can see, the Hurst exponents for the mean radius cross-correlation with meteorological parameters show lower values compared to those of the total concentation.

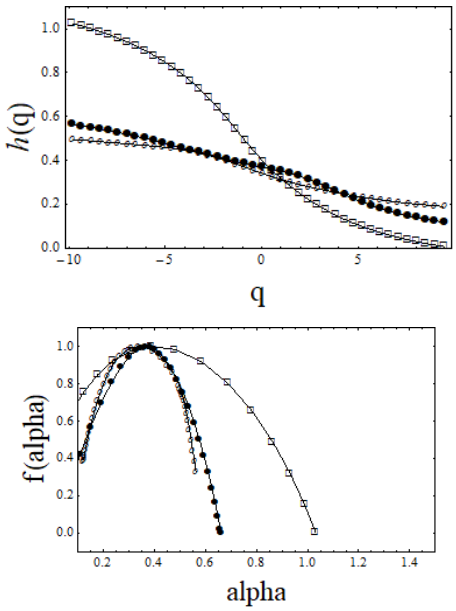

Fig. 1 – Hurst exponents dependence $h(q)$ for the total concentration of aerosols (squares), mean radius (open circles) and their cross-correlation (upper panel), and the corresponding singularity spectra (lower panel).

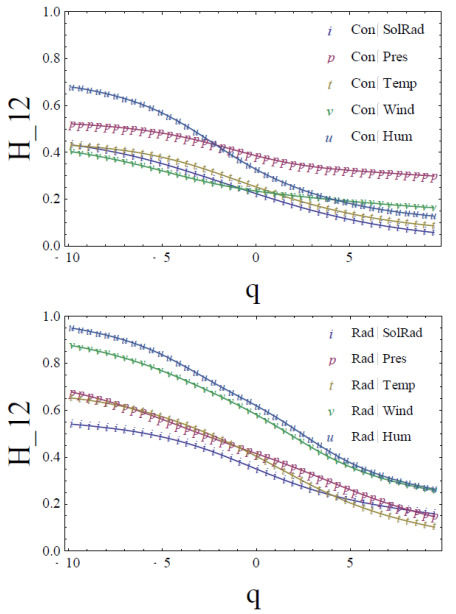

Fig. 2 – Generalized Hurst exponent for the cross-correlation between total concentration and the meteorological parameters (upper panel), and between the mean radius and the meteorological parameters (lower panel).

The curves in Fig. 2 can be easily quantified using the logistic function [26] – as the best fitting of the dependence of H_12 *versus q*

$$H\_12\ (q) = a\ /\ [1 + e^{-k\ (-c\ +\ q)}], \tag{1}$$

where a represents the curve maximum value, k stands for the steepness of the curve and c is the q value of the sigmoid midpoint.

The corresponding parameters are shown in the plots presented in Fig. 3.

In Fig. 3 and within all tables, we have arbitrarily adopted the same succession of meteo parameters in order to simplify the discussion. It is interesting to observe the shift of the values of various computed parameters when going from one meteo parameter to the next. For example, the graph of parameter a in Fig. 3 shows a shift towards a larger value when going from the SolRad parameter to the Pres one. This is true both for the particle concentration and radius.

On the contrary, when passing from the Pres parameter to the Temp one, the values corresponding to the particle concentration and particle radius are both decreasing. In the next step, when going from Temp to Wind both values are shifted towards higher values and a similar pattern is observed when passing from Wind to Hum.

In conclusion, there is a complete correlation in the shift of the a parameter for the particle concentration and particle radius when going from one meteo parameter to the next. The same situation occurs for the other logistic function parameters c and k.

It should also be noted that changes of the logistic parameters corresponding to the particle concentration and particle radius when going from one meteo parameter to the other are considerably different in magnitude. The shift is sensibly smaller in case of the mean radius dependence.

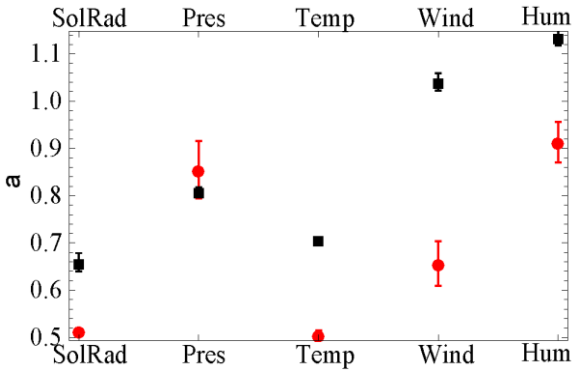

(a)

Fig. 3

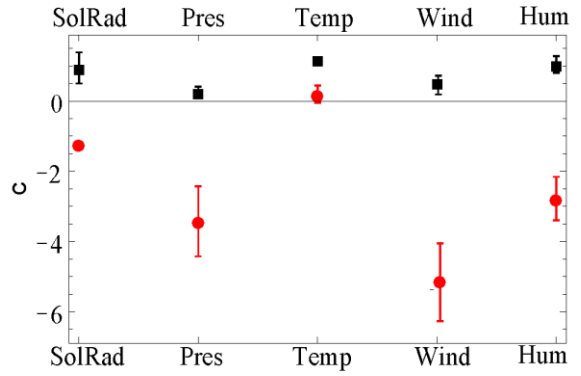

(b)

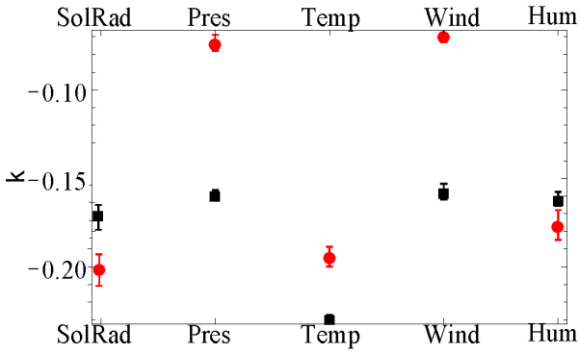

(c)

Fig. 3 (continued) – Plots of the fitting parameters a, c, k of the logistic function for the two types of cross correlation: total concentration – meteorological elements (circles) and mean radius – meteorological elements (squares).

The main Hurst exponent H_12 values computed for $q = 2$ using the logistic function are listed in Table 1.

Table 1

The main Hurst exponent H_12

H_12($q = 2$)	**SolRad**	**Pres**	**Temp**	**Wind**	**Hum**
Total Concentration	0.177	0.343	0.209	0.245	0.275
Mean Radius	0.302	0.349	0.322	0.494	0.524

As seen from Table 1, all pairs exhibit values lower than 0.5 which means anti-persistence, except the case of radius/humidity cross correlation which is larger than 0.5. In such case, the correlation between the pair humidity and mean

radius is persistent, meaning that any increase /decrease is more probably followed by a new increase/decrease of the values.

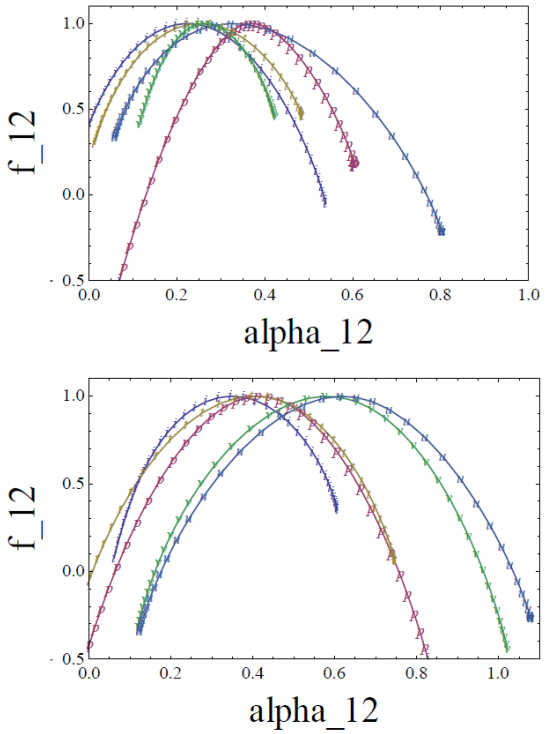

Fig. 4 – Singularity spectra for the cross-correlation between total concentration and meteorological elements (up) and between the mean radius the meteorological elements (down).

The singularity spectra in Fig. 4 show distinct characteristics, usually quantified by the main fractal dimension $\alpha(f\_12)_{max}$. The corresponding values are given in Table 2.

Table 2

Main fractal dimension

$\alpha(f\_12)_{max}$	**SolRad**	**Pres**	**Temp**	**Wind**	**Hum**
Total Concentration	0.223	0.374	0.251	0.262	0.329
Mean Radius	0.343	0.430	0.421	0.573	0.626

We shall further proceed with a similar analysis performed on the values that we input in the tables. Table 1 presents the values of the main Hurst exponent, and shows the same correlation between the parameter value shifts corresponding to particle concentration/radius when passing from one meteo parameter to the other;

besides that, a similar shift was observed as in the case of the *a* parameter of the logistic function. The situation is similar for the values of each singularity spectra maximum, as presented in Table 2.

The clear conclusion is that correlation between the meteorological conditions and total mean concentration of aerosol particles is considerably stronger than correlation between the meteorological conditions and the average particles diameter. This conclusion is in consonance with previous studies that emphasize the inter-dependence of aerosol concentrations and wind intensity, where the strong anti-correlation between them is highlighted [27].

The result should also be of relevance in the context of the dynamics of the *planetary mixing layer* (PML). The solar radiation and temperature represent a driving force in the PML due to the influence in dilution and particle concentration processes that occur during both daytime and night time. Particle dilution is especially associated to vertical air masses movement in case of low pressure systems, when high humidity is also present, while high pressure systems favour accumulation of aerosols within PML [1].

4. CONCLUSION

We apply the multifractal detrended cross-correlation analysis to characterize the relationship between total concentration of particles, their mean radius and the average values of air temperature, wind speed, solar radiation, relative humidity and absolute pressure. Numerical computations demonstrate specific characteristics for the long-range correlations as expressed by the Hurst exponents, and for the spectrum of fractal dimensions. Using the logistic function as the best fitting of the Hurst exponents *versus* the strength of fluctuations, we demonstrate that there is a complete correlation in the shift of the parameter for the particle concentration and particle radius, when going from one meteo parameter to the next.

Our numerical computations demonstrate that the presence of polluting particles has significant bearing on the main meteo parameters, while their average diameter is of secondary importance.

Acknowledgments. This work was supported by a grant of the Ministry of National Educations and Scientific Research, RDI Program for Space Technology and Advanced Research – STAR, project number 136/20.07.2017.

REFERENCES

1. J. H. Seinfeld and S. N. Pandis, *Atmospheric Chemistry and Physics: From Air Pollution to Climate Change*, Wiley (2006).
2. A. T. Lebedev, Editor. *Comprehensive Environmental Mass Spectrometry*. ILM Publications (2012).

3. M. Viana (Ed.), *Urban Air Quality in Europe*, The Handbook of Environmental Chemistry Series, **26**, Springer, 2013.
4. B. Mihalcea, Phys. Scr. T140, 014056 (2010).
5. D. G. Nash, T. Baer, and M. V. Johnston. *Aerosol mass spectrometry: An introductory review*. Int. J. Mass Spectrometry **258**, p. 2–12, 2006.
6. P. Kulkarni, P. A. Baron, K. Willeke (Eds), *Aerosol Measurement*: *Principles, Techniques, and Applications*, Wiley, 3rd Ed., 2011.
7. B. M. Mihalcea, Phys. Scr. **T135** 014006 (2009).
8. B. M. Mihalcea, G. Visan, L. C. Giurgiu *et al*., J. Optoel. Adv. Mat. **10** (8), 1994–1998 (2008).
9. B. M. Mihalcea, C. Stan, L. C. Giurgiu *et al*., Rom. Journ. Phys. **61** (7–8), 1395–1411 (2016)
10. J. W Kantelhardt, S. A. Zschiegner, E. Koscielny-Bunde *et al*., Physica A **316**, 87–114 (2002).
11. S. Lovejoy, D. Schertzer, Comput.Geosci. **36**, 1393 (2010).
12. M. S. Movahed, G. R. Jafari, F. Ghasemi *et al*., J. Stat. Mech. 0602, P02003 (2006).
13. C. Stan, M. T. Cristescu, L. I., Buimaga *et al*., J.Theor. Bio, 321, 54-62 (2013).
14. L. Kristoufek, Phys. Rev. E **90**, 062802 (2014).
15. C. P. Cristescu, C. Stan, E. I. Scarlat, UPB Sci Bull Ser A **69**, 37−44 (2007).
16. K. Shi, C. Q. Liu, Atmos. Environ. **43**, 3301–3304 (2009).
17. K. Shi, C. Liu, Y. Huang, Aerosol Air Qual. Res. **15**, 926–934 (2015).
18. N. Yuan, Z. Fu, J. Mao, Theor Appl Climatol **112**, 673−682 (2013).
19. H. L. Windsor, R. Toumi, Atmos. Environ. **35**, 4545–4556 (2001).
20. C. K Lee, L. C. Juang, C. C. Wang *et al*., Chemosphere **62**, 934–946 (2006).
21. C. Zhang, Z. W. Ni, L. P. Ni, Physica A **438**, 114–23 (2015).
22. X. Wang, Y. Mei, W. Li, Y. Kong, X. Cong, PLoSONE **11**, e0146284. (2016)
23. Y. Xue, P. Wei, L. Wei-Zhen, H. Hong-Di, Sci. Total Environ. **532**, 744–751 (2015).
24. P. Baranowski, J. Krzyszczak, C. Slawinski *et al.*, Clim Res **65**, 39–52 (2015).
25. W.-X. Zhou, Phys. Rev. E **77**, 066211 (2008).
26. C. Stan, M. Balasoiu, D. Buzatu, C.P. Cristescu, J. Comput. Theor. Nanosci. **14**, 2030–2034 (2017).
27. A. Bigi, G. Ghermandi, R. M. Harrison, J. Environ. Monit., 14, 552–563 (2012).